Structural and conformational properties of a quasi-two-dimensional dipolar fluid

2002 J. Phys.: Condens. Matter 14 9171

(http://iopscience.iop.org/0953-8984/14/40/310)

INSTITUTE OF PHYSICS PUBLISHING JOURNAL OF PHYSICS: CONDENSED MATTER

J. Phys.: Condens. Matter **14** (2002) 9171–9186 PII: S0953-8984(02)36381-1

Structural and conformational properties of a quasi-two-dimensional dipolar fluid

J J Weis[1], J M Tavares[2,3] and M M Telo da Gama[2]

[1] Laboratoire de Physique Théorique, Université de Paris XI, Bâtiment 210, F-91405, Orsay Cedex, France
[2] Centro de Física da Matéria Condensada da Universidade de Lisboa, Avenida Professor Gama Pinto 2, P-1649-003 Lisbon, Portugal
[3] Universidade Aberta, Rua Fernão Lopes, 9, 2 D, P-1000-132 Lisbon, Portugal

Received 30 April 2002
Published 27 September 2002
Online at stacks.iop.org/JPhysCM/14/9171

Abstract

A survey of the structural properties of a quasi-two-dimensional dipolar fluid is given with emphasis on the low-density regime where particles self-assemble into clusters. The internal energy, conformational properties and equilibrium length distributions of the clusters are measured by means of Monte Carlo simulation and compared with equilibrium polymer theory. The scaling forms of the length distribution functions predicted by theory are found to describe the simulation results adequately. The existence and mechanisms of phase transitions in dilute dipolar fluids are discussed.

1. Introduction

Dipolar interactions play an essential role in determining the structural properties of a variety of two-dimensional (2D) magnetic or electrical systems as illustrated by the following few examples:

(i) The long-range dipolar forces stabilize, at finite temperature, long-range orientational order in 2D ferromagnets [1–3]. Spontaneous long-range order does not occur if only exchange interactions are present, as the ground state is unstable against low-energy spin-wave excitations [4].
(ii) In ultrathin magnetic films, interplay between the dipolar interaction, favouring in-plane orientation of the spins, and uniaxial surface anisotropy perpendicular to the film layer, favouring out-of-plane orientation, can give rise to a reorientational transition where the magnetization of the system changes from parallel to the film to perpendicular to the film [5–7].
(iii) If the spins are aligned predominantly perpendicular to the magnetic film surface, competition between the repulsive long-range dipolar interaction and the attractive short-range exchange interaction can lead to the spontaneous formation of modulated structures such as stripes and bubbles (circular droplets in 2D [5, 8, 9]).

Of similar origin is pattern formation observed in phospholipid monolayers at the water–air interface where it arises through the competition between the perpendicular component of the dipole of the polar head group at the interface and the short-range van der Waals interaction [10–14] or in thin films of magnetic garnets [15–17], but appears also in type I superconducting films [18], diblock copolymers [9] etc.

Experimental magnetic monolayers or few-layer systems can be realized by growth of metal films on metal substrates or films of rare-earth systems [5] or by deposition of Co nanoparticles on a substrate [19–22] and also by confining microsized or millisized magnetic or dielectric particles between glass plates [23] or on a water/air interface [24] or letting them float on a liquid surface [25] or meniscus [26]. When, in the latter cases, an electric or magnetic field is applied perpendicular to the sample, the dipolar particles experience a repulsive $1/r^3$ potential and self-assemble into crystalline structures. Melting of the dipolar solid could be investigated in this way and shown to be consistent with the KTHNY scenario [27–29]. Monodisperse polystyrene spheres (1–100 μm) dispersed in a ferrofluid (0.01 μm) confined between closely spaced parallel glass plates provide another convenient way to study order–disorder phenomena in magnetic monolayers [30–32]. In an external field the non-magnetic spheres (magnetic holes) acquire an effective magnetic moment corresponding to that of the displaced ferrofluid and collinear with the external field. In a perpendicular field, the spheres crystallize in a triangular lattice, whereas in a field parallel to the surface, attractive dipolar interactions trigger formation of linear chains and aggregation of the chains.

Lattice Monte Carlo (MC) simulations [5, 33–45] and theoretical investigations [5, 46–52] based on a Hamiltonian comprising a long-range dipole–dipole interaction, a nearest-neighbour exchange interaction and a local magnetocrystalline (surface) anisotropy [53, 54] have provided qualitative insight into the phenomena of reorientation transitions and pattern formation of model thin magnetic films.

The purpose of this paper is to present a survey of the structural properties, as obtained from computer simulation and theory, of perhaps the simplest model of a quasi-2D system of magnetic spheres, namely quasi-2D dipolar hard spheres [45, 55–59].

The quasi-2D dipolar hard-sphere model is a system of hard spheres (discs) of diameter σ with an embedded point dipole of strength μ interacting through the pair potential

$$u(\boldsymbol{r}_{ij}, \boldsymbol{s}_i, \boldsymbol{s}_j) = \begin{cases} \infty & r_{ij} < \sigma \\ \dfrac{\mu^2}{r_{ij}^3}\left[\boldsymbol{s}_i \cdot \boldsymbol{s}_j - \dfrac{3(\boldsymbol{s}_i \cdot \boldsymbol{r}_{ij})(\boldsymbol{s}_j \cdot \boldsymbol{r}_{ij})}{r_{ij}^2}\right] & r_{ij} \geqslant \sigma . \end{cases} \tag{1}$$

In the system the centres of the spheres are confined to a plane and therefore $\boldsymbol{r}_{ij} = \boldsymbol{r}_j - \boldsymbol{r}_i$ joining particles i and j is a two-component vector lying in the confining plane. The dipole moments, represented by unit vectors $\boldsymbol{s}_i$ and $\boldsymbol{s}_j$, can rotate in full 3D space. With decreasing temperature the dipole moments show, however, an increased tendency to lie on the plane and most of our results described below pertain to the case where the dipole moments are restricted to rotating in the plane.

The structural properties described in sections 2 and 3 are obtained from off-lattice MC simulations and cover the density range $0.025 \leqslant \rho^* \leqslant 1.05$, from gas to solid, and the temperature range $0.11 \leqslant T^* \leqslant 0.16$. The reduced density is defined as $\rho^* = \sigma^2 N/A$ (N number of particles, A area of the simulation box) and the reduced temperature as $T^* = kT\sigma^3/\mu^2$ (k is the Boltzmann constant). It is also convenient to define a reduced dipole moment $\mu^* = \mu/\sqrt{\sigma^3 kT}$.

The MC simulations were performed in the canonical (NVT) ensemble using 5760 (5776) particles in a rectangular (square) box with periodic boundary conditions. A Ewald sum was used to account for the long range of the dipole–dipole interaction [45, 60]; for a 3D dipolar

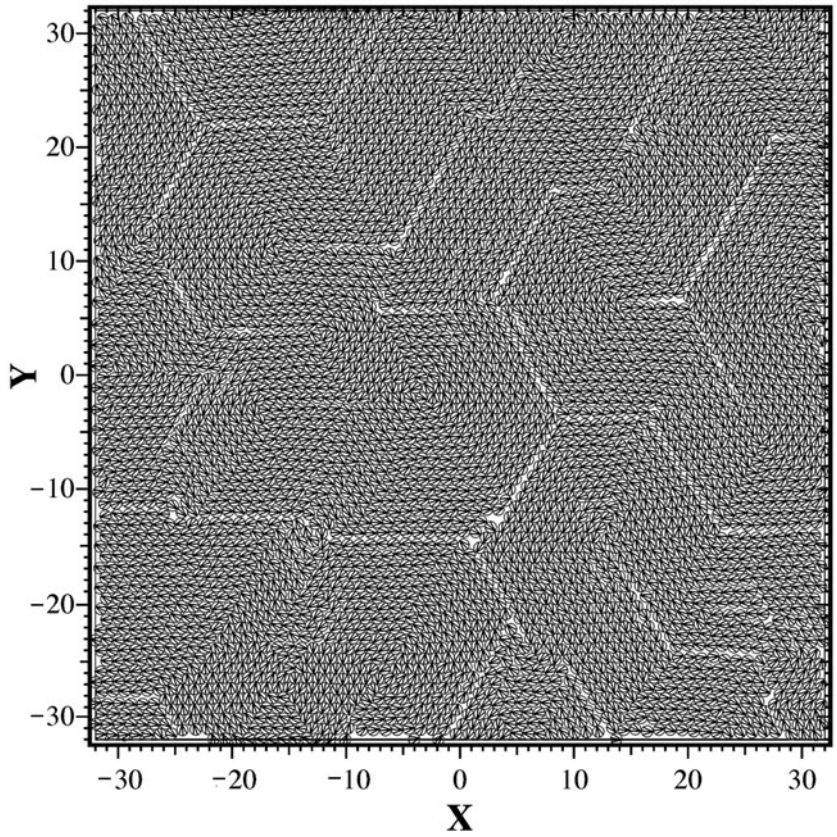

Figure 1. A snapshot of a configuration of 5760 dipoles at $\rho^* = 1.05$, $\mu^* = 3$ on a periodic hexagonal lattice of dimensions $L_x = 75.5$, $L_y = 72.7$ (in units of σ). Arrows represent the projections of the dipole moments on the xy-plane. Only the central part of the system is shown.

interaction with the centres of the spheres constrained to a 2D lattice, the sum is absolutely convergent. Sampling of configurations involves single-particle and, at low density, also cluster moves.

The main emphasis will be given to the low-density states where the dipolar particles associate into chains, rings and more complicated structures whose properties will be described using equilibrium polymer theory [61, 62]. In particular, the scaling predicted theoretically is compared with that observed for the simulated length distributions of chains and rings.

2. Orientational ordering at high density

Snapshots of configurations of dipolar spheres showing the orientational order in the high-density solid state are presented in figure 1 for an infinite hexagonal lattice ($\rho^* = 1.05$) and in figure 2 for an infinite square lattice ($\rho^* = 0.99$). At the dipole strength considered, $\mu^* = 3$, the dipole moments lie predominantly in plane and form faceted domains with edges along the lattice (simulation cell) axes. For a hexagonal system the domains are of hexagonal shape and within them the dipoles orient in a vortex-like structure. Dipoles along edges run in opposite directions. For the state considered, the size of the domains is approximately 20 σ. On a

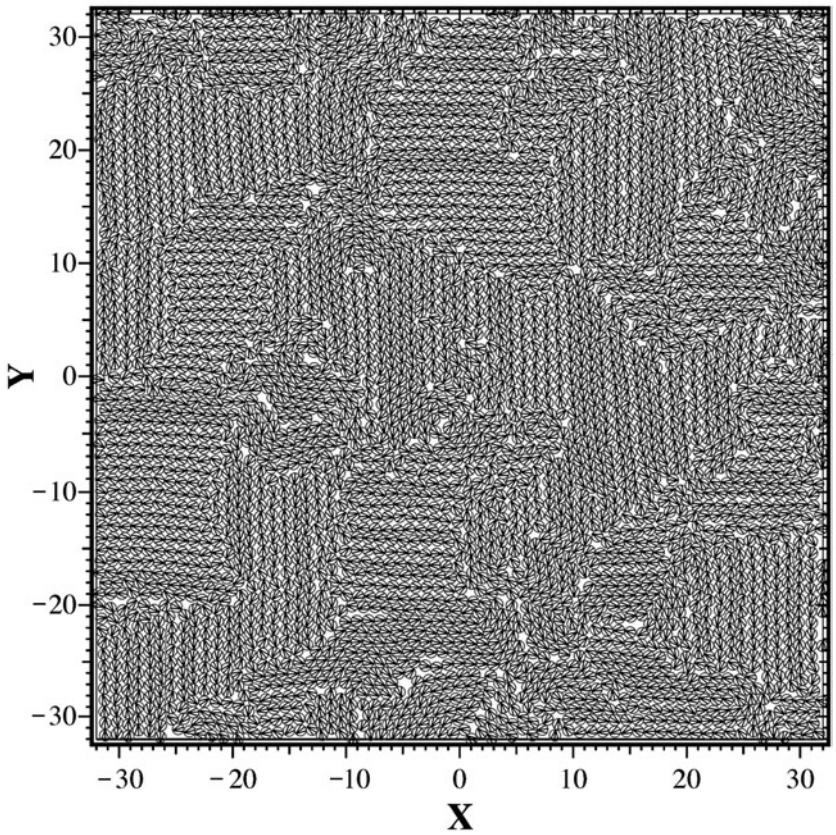

Figure 2. A snapshot of a configuration of 5776 dipoles at $\rho^* = 0.99$, $\mu^* = 3$ on a periodic square lattice of dimensions $L_x = L_y = 76.4$ (in units of σ). The dipoles are assumed to lie in the plane. Only the central part of the system is shown.

square lattice the system breaks up into irregular more or less rectangular domains within which the dipoles organize into rows roughly parallel to the x- or y-axis of the simulation cell. Dipole moments in different rows can point in the same or opposite directions. Lattice MC simulations have shown that in-plane dipoles on a square lattice order below a non-zero critical temperature [2]. In the present simulations no net magnetization of the system is observed at the temperature considered.

When the density of the system is lowered below the melting density and the dipoles progressively get less packed, they organize into large linear structures percolating through the simulation cell with a strong tendency to form loops (cf figures 3 and 4). Only at a density $\rho^* \leqslant 0.15$ (at $\mu^* = 2.75$–3) do the dipolar spheres self-assemble into aggregates of different sizes.

3. Cluster structure at low density

As is evident from a snapshot of an equilibrium configuration at $\rho^* = 0.031\,25$ and dipole moment $\mu^* = 2.75$ (figure 5), these low-density aggregates can have linear structure (every particle is bonded to at most two other particles), closed (rings) or open (chains), or be more complex and exhibit branching, even if most of their particles are still linearly aggregated. These branching points are called defects and the structures that they belong to defect clusters,

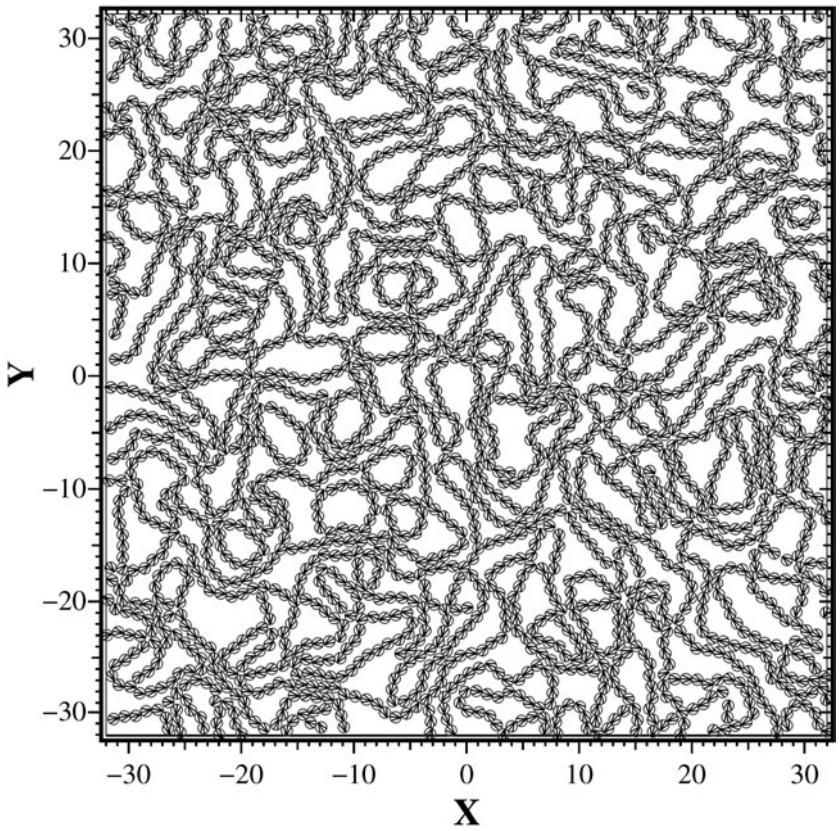

Figure 3. A snapshot of a configuration of 5760 dipoles at $\rho^* = 0.6$, $\mu^* = 3$ in a rectangular box of dimensions $L_x = 99.9$, $L_y = 96.1$ (in units of σ). Arrows represent the projections of the dipole moments on the xy-plane. Only the central part of the system is shown.

irrespective of their topology. The defects exhibit a different number of branches (mostly 3 or 4, called Y and X defects, respectively, following [63, 64]) and the corresponding clusters exhibit different topologies, depending on the number of 'holes' and 'ends' and on the type of defect.

These clusters evolve by breaking and recombining, the relative concentration of chains, rings and defect clusters and their sizes depending on density and temperature. To quantify these aspects a classification of clusters has been carried out by calculating the first-, second- and third-nearest-neighbour distances (respectively, r_{1j}, r_{2j} and r_{3j}) for each particle j: if $r_{1j} > r_c$, then j is a free particle; if $r_{1j} < r_c$ and $r_{2j} > r_c$, then j is an end particle; if $r_{2j} < r_c$ and $r_{3j} > r_c$, then j is an interior particle; and, finally, if $r_{3j} < r_c$, then j is a defect particle. A ring is a cluster with interior particles only, a chain a cluster with two (and only two) ends and a defect cluster a cluster with at least one defect particle. For strongly bonded clusters (as occur in the present system) a range of cut-off distances yield qualitatively similar results. Throughout this work we used $r_c = 1.15\,\sigma$.

3.1. Simulation results

Cluster properties, internal energy, length distribution and conformations have been analysed for densities in the range $0.025 \leqslant \rho^* \leqslant 0.0375$ and dipole moments between $\mu^* = 2.5$ and 3. In this section the dipole moments are assumed to lie on the plane.

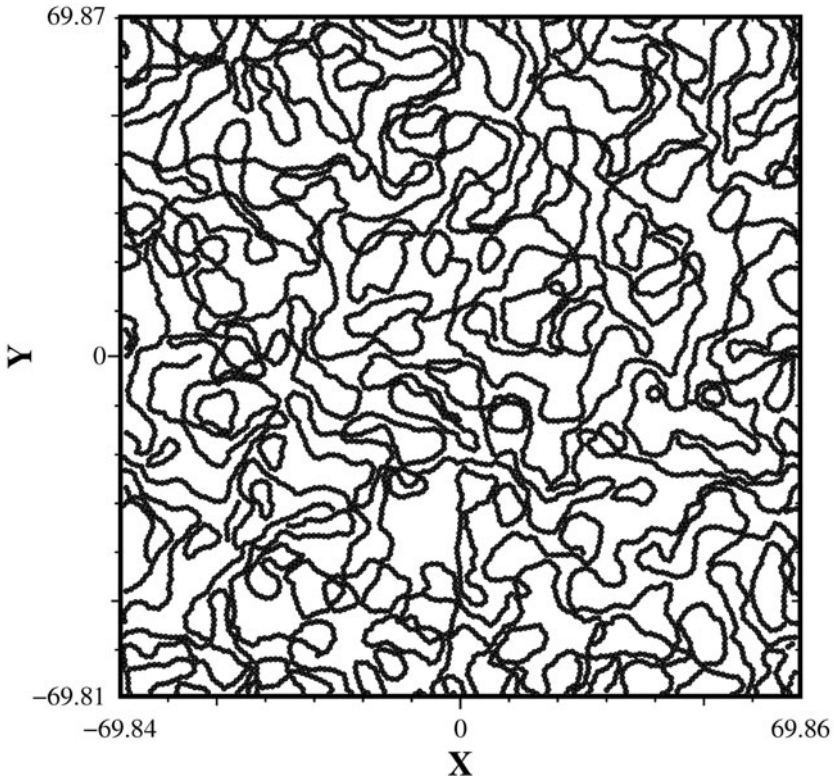

Figure 4. A snapshot of a configuration of 5776 dipoles at $\rho^* = 0.3$, $\mu^* = 2.75$ in a square box of dimensions $L_x = L_y = 138$ (in units of σ). The dipoles are assumed to lie in the plane.

An example of the length distribution of chains, rings and defect clusters is shown in figure 6 for $\rho^* = 0.031\,25$ and $\mu^* = 2.75$. Distributions of similar shape occur for all other thermodynamic states, suggesting scaling behaviour (see below). Overall, the mean length of chains, rings and defect clusters increases with density and dipole moment, though at different rates, while the fraction of particles decreases in favour of those in defect clusters. For a more quantitative analysis we refer the reader to [59].

The reduced total internal energy per particle U/NkT, divided by μ^{*2}, decreases slightly with increasing dipole moment and is practically independent of density, indicating that intercluster interactions are negligible. This is corroborated by a direct calculation of the average internal energy per particle in clusters, which was found to be nearly the same as the total internal energy per particle.

The internal energy per particle of each type of cluster has been computed as a function of size N. An example is given in figure 7 for $\rho^* = 0.031\,25$ and $\mu^* = 2.75$. For all the states considered the energy of rings, $\epsilon_r(N)$, is lower than that, $\epsilon_c(N)$, of chains if $N \geqslant 4$ and the difference $\epsilon_r(N) - \epsilon_c(N)$ exhibits a minimum for $N \approx 8$–10. The internal energy of defect clusters is always larger than that of rings and it appears to be larger than that of chains for small N only, though a definite conclusion must await more precise simulation results.

In line with zero-temperature results [65], $\epsilon_c(N)$ and $\epsilon_r(N)$ are well approximated (except for the smallest values of N) by the functions

$$\frac{\epsilon_c(N)}{\mu^{*2}kT} = -\epsilon_0^c + \frac{\epsilon_1^c}{N}, \tag{2}$$

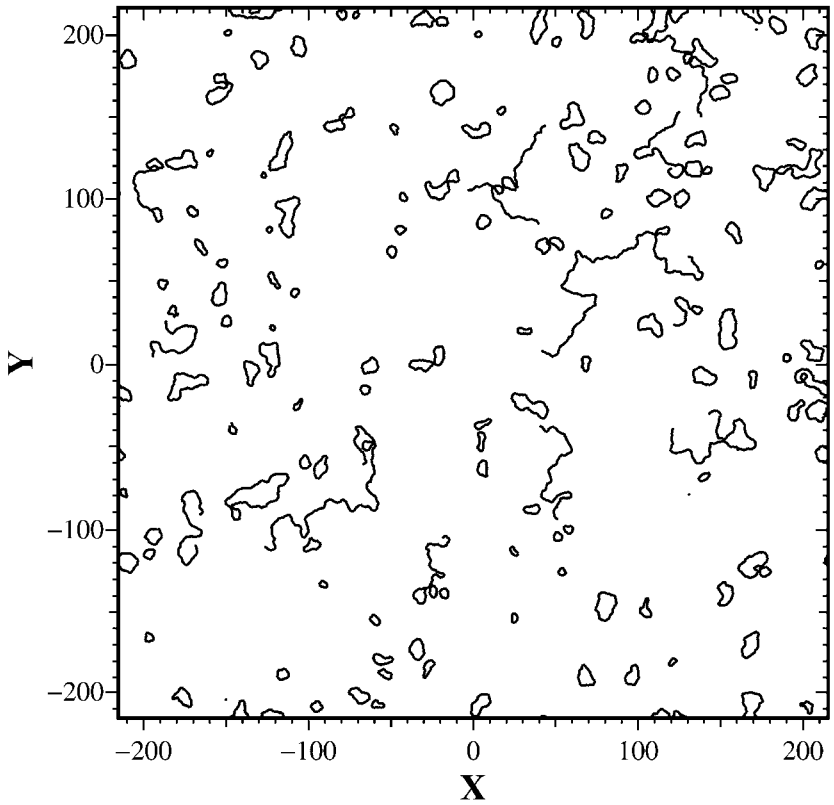

Figure 5. A snapshot of a configuration of 5776 dipoles at $\rho^* = 0.031\,25$, $\mu^* = 2.75$ in a square box of dimensions $L_x = L_y = 430$ (in units of σ). The dipoles are assumed to lie in the plane.

Table 1. Parameters of the internal energy for rings and chains.

μ^*	ϵ_0	ϵ_1^c	ϵ_1^r
2.5	2.05	2.56	10 ± 1
2.75	2.12	2.65	11 ± 1
3.0	2.17	2.66	12 ± 1

and

$$\frac{\epsilon_r(N)}{\mu^{*2}kT} = -\epsilon_0^r + \frac{\epsilon_1^r}{N^2}. \tag{3}$$

The coefficients ϵ_0^c, ϵ_0^r, ϵ_1^c and ϵ_1^r have been determined by fitting the simulation data to equations (2) and (3) and are collected in table 1. Their dependence on density is found to be negligible (in the range considered) and, in addition, for a given temperature, ϵ_0^c and ϵ_0^r differ by less than 1% which allows an assignment of a well defined bond energy, $\epsilon_0(\mu^*) = \epsilon_0^c(\mu^*) = \epsilon_0^r(\mu^*)$, to the system. Figure 7 includes a comparison of the variation of $\epsilon_c(N)$ and $\epsilon_r(N)$ with cluster size obtained from the simulations and the functions (2) and (3) calculated using the parameters of table 1.

Conformational properties of the clusters were obtained from the calculation of the radius of gyration and persistence length. For large N, the radius of gyration R_g of the clusters scales

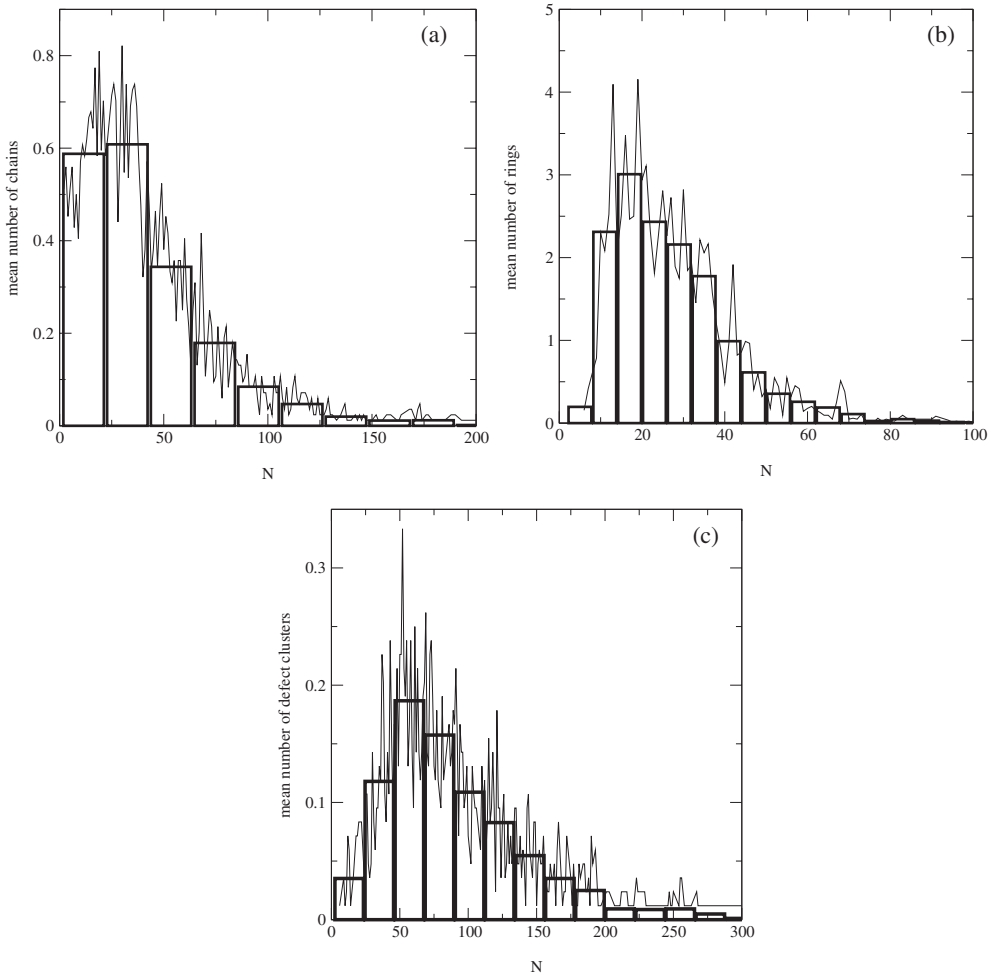

Figure 6. The average number of clusters of size N obtained from simulations at $\rho^* = 0.031\,25$, $\mu^* = 2.75$: (a) chains, (b) rings, (c) defect clusters.

with the number of monomers N as

$$R_g(N) = bN^{\nu}, \tag{4}$$

where b is a characteristic length and ν a universal exponent that depends on the dimension of space and on the type of interaction. For rigid objects $\nu = 1$ and for random walks 0.5. Clusters with the conformation of a self-avoiding random walk (SARW) in 2D have $\nu = 0.75$ [62, 66]. The mean value of the radius of gyration squared $\langle R_g^2(N)\rangle$ for chains and rings of length N obtained from the simulations is shown in figure 8 for $\rho^* = 0.031\,25$ and $\mu^* = 2.75$. It is clear from figure 8 that $\nu = 0.75$ for long chains (N greater than $\approx$10) and thus dipolar chains have the conformation of a 2D SARW. Similar results were obtained for all the other simulations and we conclude that the exponent is universal in the range of densities and dipole moments considered in this work.

For rings, the scaling regime of SARWs with return to the origin (characterized by the same exponent $\nu = 0.75$) is observed for rings larger than $N \approx 40$) (cf figure 8). Smaller rings

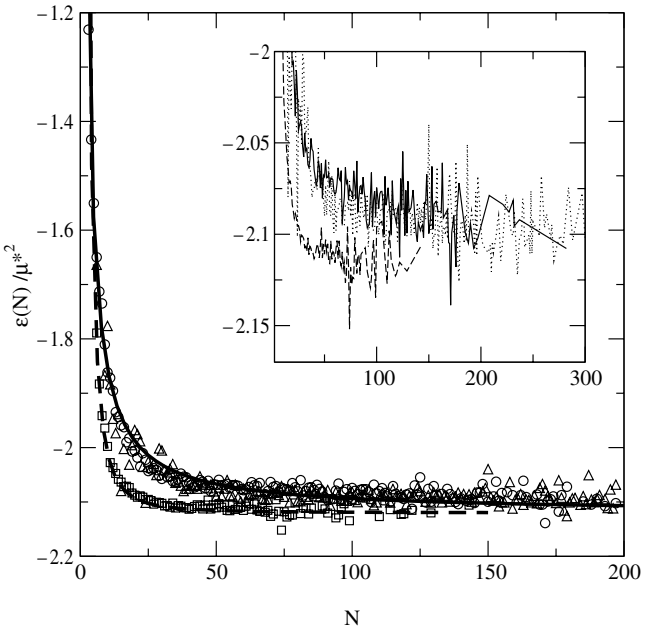

Figure 7. The energy per particle (divided by $\mu^{*2}kT$) for chains (circles), rings (squares) and defect clusters (triangles) of length N from simulations at $\rho^* = 0.031\,25$, $\mu^* = 2.75$. In the main figure the curves are fits to the simulation data obtained using equations (2) and (3) and the values of table 1. The inset shows the tails in more detail: the full curve corresponds to chains, the dashed curve to rings and the dotted curve to defect clusters.

scale with ν close to 1, indicating that they behave as rigid objects. The crossover from the rigid to the fluctuating SARW regime is broader at higher temperatures and lower densities.

For given density and temperature the persistence length of chains, $\ell_c(N)$, is found to be constant within the statistical error while that of rings, $\ell_r(N)$, displays two regimes: it increases linearly with N at small N reaching a constant value at large N. The crossover between the rigid and SARW regimes occurs at larger values of N at lower temperatures [59].

3.2. Scaling laws: equilibrium polymers theory

Well defined length distribution and bonding energy of all the clusters and negligible intercluster interaction suggest that the quasi-2D dipolar fluid may be described as an ideal mixture of various types of cluster in chemical equilibrium [67, 68]. The Helmholtz free energy density, F/A, of this system is written as

$$\sigma^2 F/AkT = \sum_k \sum_{N=s_k}^{\infty} \rho_k^*(N)(\ln \rho_k^*(N) - 1 - \ln \tilde{q}_k(N)), \tag{5}$$

where k labels the type of cluster (chains, rings and the several types of defect cluster), s_k is the minimal length of clusters of type k, while $\tilde{q}_k(N)$ is the partition function (multiplied by σ^2/A) and $\rho_k^*(N)$ the reduced density of clusters of type k with length N. Minimization of the free energy with respect to the densities $\rho_k^*(N)$ yields the set of equations

$$\rho_k^*(N) = \tilde{q}_k(N) \exp(N\beta\mu), \tag{6}$$

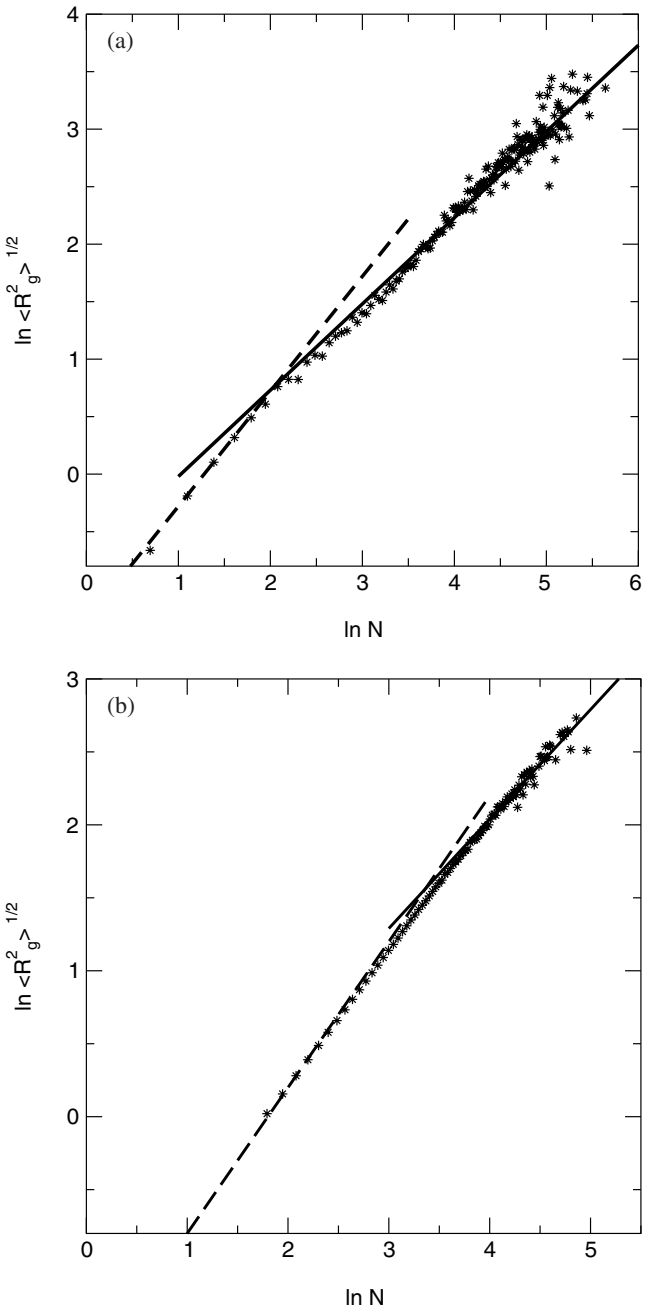

Figure 8. Radius of gyration (in units of σ) as a function of the number of monomers in (a) chains and (b) rings at $\rho^* = 0.031\,25$, $\mu^* = 2.75$: the full line has slope 0.75 and the dashed line slope 1.

where μ is the chemical potential of the system and $\beta = 1/kT$. The cluster densities satisfy the condition

$$\rho^* = \sum_k \sum_{s_k}^{\infty} N\rho_k^*(N), \tag{7}$$

and may be viewed as length distributions for the various types of cluster. Given the cluster partition functions, $\tilde{q}_k(N)$, these equations determine the structure and thermodynamics of the system.

The results for the conformational properties of dipolar chains and rings and the existence of chemical equilibrium among clusters suggest that these aggregates behave as dilute equilibrium polymers. In the following we will show, by comparing theoretical and simulation results, that the conformational properties of dipolar chains and rings are in accord with predictions of equilibrium polymer theory.

Thus we approximate the partition function of an isolated dipolar chain with N monomers of diameter σ by the product of two terms:

(i) the number of conformations of a SARW with N steps, in the limit $N \to \infty$ [62]; and
(ii) the Boltzmann factor of the energy $E_c(N)$ [69, 70]:

$$Z_c(N) = A_c N^{\gamma-1} \exp(-\beta E_c(N)). \tag{8}$$

γ is a universal exponent that depends on the dimension of space and on the type of interaction and A_c is a non-universal constant. Substituting this result into equation (6) and using equation (2) we find for the reduced density of non-interacting, N-dipolar chains

$$\rho_c^*(N) = A_c N^{\gamma-1} \exp(-\epsilon_1^c \mu^{*2} - \tilde{\mu} N), \tag{9}$$

where $\tilde{\mu} = -\beta\mu - \epsilon_0 \mu^{*2}$ is the shifted chemical potential. Comparison of the chain densities obtained from the simulations with those calculated using equation (9) requires an approximation for the (shifted) chemical potential, $\tilde{\mu}$. This is achieved by approximating the chain density (9) by a continuous function, namely a non-normalized gamma distribution. The first moment of this distribution yields

$$\bar{N}_c \equiv \frac{\sum_{N=2}^{\infty} N\rho_c^*(N)}{\sum_{N=2}^{\infty} \rho_c^*(N)} \approx \frac{\int_0^{\infty} N\rho_c^*(N)\,\mathrm{d}N}{\int_0^{\infty} \rho_c^*(N)\,\mathrm{d}N} = \frac{\gamma}{\tilde{\mu}}. \tag{10}$$

relating $\tilde{\mu}$ to the inverse of the mean chain length $\bar{N}_c$.

With the use of equation (10) the *normalized* distribution of chains $\Phi_c(N)$ corresponding to (9) should scale as

$$\ln(N\Phi_c(N)) = \gamma \ln\gamma - \ln\Gamma(\gamma) + \gamma\left(\ln\frac{N}{\bar{N}_c} - \frac{N}{\bar{N}_c}\right), \tag{11}$$

where $\Gamma(x)$ is the gamma function. Figure 9 shows that the scaling form applies to intermediate values of $N/\bar{N}_c$. The scaling region is wider at low dipole moments and densities, in line with the fact that deviations from scaling for large N are due to statistical noise.

Similarly to in the chain case we approximate, in accord with equilibrium polymer theory, the partition function of isolated, long, N-monomer dipolar rings by the product of two terms:

(i) the number of conformations of a SARW of N steps with return to the origin, in the limit $N \to \infty$ [62]; and
(ii) the Boltzmann factor of the energy $E_r(N)$ [70].

In addition, as remarked in [70], equilibrium between chains and rings has to be taken into account by including the possibility that N-rings may break in N different places yielding an N-chain. The partition function of an N-ring is then

$$Z_r(N) = A_r N^{\alpha-3} \exp(-\beta E_r(N)). \tag{12}$$

where A_r is a non-universal constant and α a universal exponent obeying the hyperscaling relation, $\alpha = 2 - \nu D$, and thus $\alpha = 0.5$ for a SARW with $D = 2$. Substitution of this equation

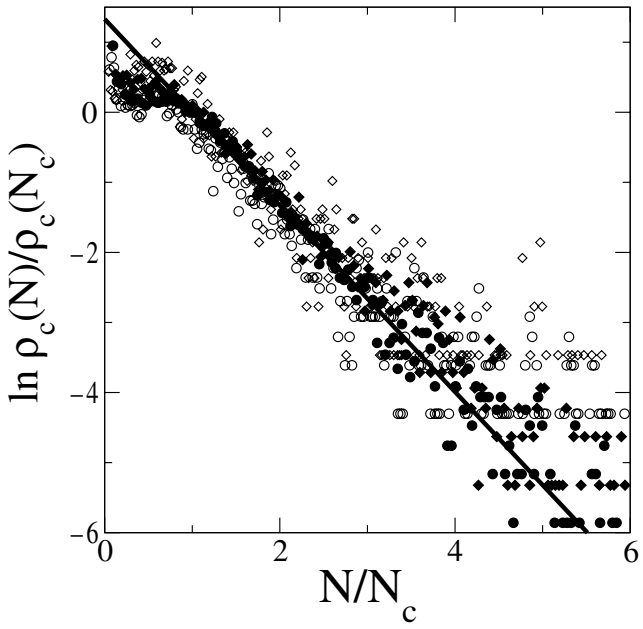

Figure 9. The scaling form for the length distribution of dipolar chains obtained using equation (14). Circles: $\rho^* = 0.025$. Squares: $\rho^* = 0.031\,25$. Diamonds: $\rho^* = 0.0375$. Full symbols: $\mu^* = 2.5$. Open symbols: $\mu^* = 2.75$. The full line is the theoretical prediction obtained from equations (9)–(11) with $\gamma = 1.33$.

into equation (6) and use of equation (3) yields for the densities of non-interacting N-dipolar rings

$$\rho_r^*(N) = A_r N^{\alpha-3} \exp\left(-\frac{\epsilon_1^r \mu^{*2}}{N} - \tilde{\mu} N\right). \tag{13}$$

Comparison of the simulation and theoretical results is carried out for the distribution $\Phi_r(N)$ defined by

$$\Phi_r(N) = \frac{\rho_r^*(N)}{\rho_r^*(\bar{N}_c)} \exp\left(\epsilon_1^r \mu^{*2}\left(\frac{1}{N} - \frac{1}{\bar{N}_c}\right)\right). \tag{14}$$

By combining this expression with equations (13) and (10) one finds that $\Phi_r(N)$ is a universal function of $N/\bar{N}_c$, namely

$$\ln \Phi_r(N) = \gamma + (\alpha - 3) \ln \frac{N}{\bar{N}_c} - \gamma \frac{N}{\bar{N}_c}. \tag{15}$$

In figure 10 we plot $\Phi_r(N)$ (equation (14)), obtained from simulations at six different state points, and compare with the right-hand side of equation (15) calculated with $\alpha = 0.5$ and $\gamma = 1.33$. The data collapse is remarkable. The simulation results scale according to the theoretical predictions for values of N between $\bar{N}_c$ and $3\bar{N}_c$. For small N, scaling is not observed, in line with the results for the conformational properties. Statistical errors inherent in the simulations of the largest clusters prevent us from reaching a firm conclusion about scaling in the large-N limit.

By dividing $\Phi_r(N)$ by the equilibrium chain length distribution, the exponential dependence of the ring distribution function can be eliminated, to give a slowly varying scaling

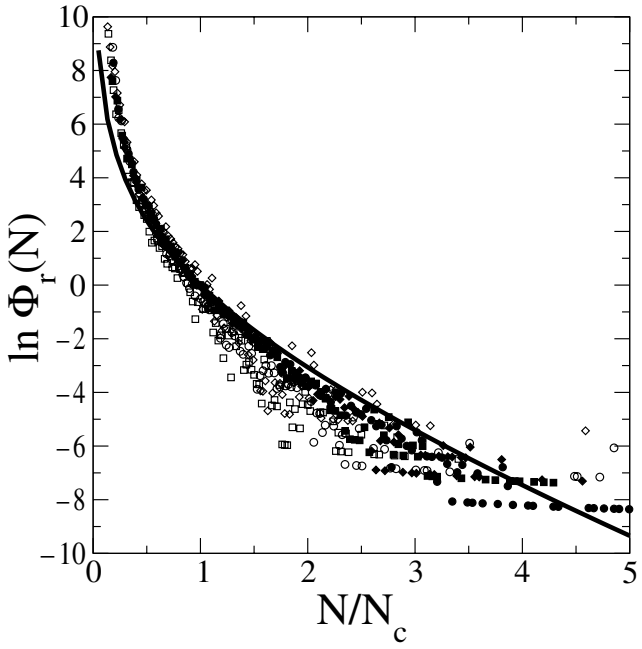

Figure 10. The scaling form for the length distribution of dipolar chains from equation (15). The full curve is the theoretical prediction (rhs of equation (15) with $\gamma = 1.33$ and $\alpha = 0.5$). The symbols are as in figure 9.

function:

$$\ln\left(\frac{\Phi_r(N)\rho_c^*(\bar{N}_c)}{\rho_c^*(N)}\right) = (\alpha - \gamma - 2)\ln\frac{N}{\bar{N}_c}, \tag{16}$$

which is plotted in figure 11. The data collapse for the six simulation runs is again remarkable. The scaling behaviour of this function is similar to that of $\Phi_r(N)$. The slope of the straight line in figure 11 is consistent with $\alpha = 0.5$, thus confirming the analogy between dipolar rings and equilibrium ring polymers. Again, departures from the straight line at small N can be traced to the crossover from rigid to flexible rings that occurs at relatively large values of N.

4. Conclusions and discussion

Our results show that the structure of the low-density quasi-2D dipolar fluid is, to a good approximation, the same as that of 2D equilibrium polymers. A major question concerning dilute strongly dipolar fluids is the existence (and nature) of a fluid–fluid phase transition in this regime. For 3D dilute dipolar systems, MC simulations in the isobaric and grand canonical ensembles and free energy calculations in the canonical ensemble suggested the existence of one (or two) isotropic fluid–fluid transitions at low densities [71, 72]. These results lead Tlusty and Safran [63] to propose a new mechanism for the phase transition of dipolar fluids at low densities and temperatures: the competition between a (low-density) phase rich in chains and entropically favourable, and a (higher-density) phase rich in defects (the junction of three chain ends and thus called Y defects [64]) and energetically favourable. A comparison of the structure observed in simulations of dipolar fluids with that responsible for the mechanism

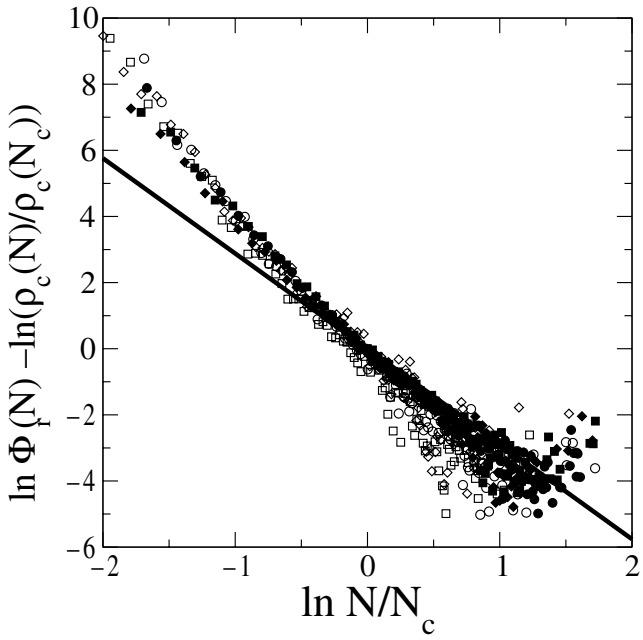

Figure 11. The scaling form for the length distribution of dipolar chains from equation (16). The full line is the theoretical prediction (rhs of equation (16) with $\gamma = 1.33$ and $\alpha = 0.5$). The symbols are as in figure 9.

proposed in [63] has not been carried out and thus the existence and mechanisms of the phase transition in 3D dilute dipolar fluids remain open problems.

The type of analysis developed in this paper, if extended to simulations at higher densities, may shed light on these questions. In fact, the mean chain and ring lengths are monotonic increasing functions of the chemical potential (see equation (10) and the definition of $\tilde{\mu}$) and depend on the total density ρ through μ only. Thus, at fixed temperature, an instability signalled by $\left(\frac{\partial \mu}{\partial \rho}\right)_T < 0$ may occur if $\bar{N}_c$ and $\bar{N}_r$ decrease in the same range of increasing densities. In other words, within simulation results as reported in this paper, the (mean-field) loops that signal first-order phase transitions correspond to loops in the mean chain and ring lengths. This type of analysis has an advantage over the direct calculation of the free energy in making a connection between the structure and the thermodynamics of the system, thus revealing the mechanism that drives the phase transition. In fact, a necessary condition for the decrease of $\bar{N}_c$ and $\bar{N}_r$ with increasing density is the self-assembly of defect clusters. This conclusion is supported by the results of [70] for linear equilibrium polymers (chains and rings) where both these quantities are shown to increase with density at all simulated temperatures. Thus, the appearance of such loops indicates the existence of a topological phase transition [63] resulting from the competition between structures with high energy and high entropy (chains) and structures with low energy and low entropy (defect clusters). Preliminary simulation results extending the density range to $\rho^* = 0.2$ at reduced dipole moment $\mu^* = 2.75$ suggest that $\bar{N}_c$ and $\bar{N}_r$ may go through a maximum near $\rho^* \sim 0.07$ (cf table 2) although, due to the rapid decrease in number of chains and rings with increasing density, better statistics is required for drawing a firm conclusion.

Other mechanisms for a phase transition which could be envisaged include a percolation transition [73] and a Bose–Einstein condensation (BEC) type of transition [74, 75].

Table 2. Structure and energy of the quasi-2D dipolar fluid obtained from simulations at $\mu^* = 2.75$ with total number of particles $N = 5776$; $U^* = \frac{U}{NkT}$ is the total reduced energy per particle, $\bar{N}_x$ is the mean length of the distribution for clusters of type x, ϕ_x is the fraction of particles in clusters of type x, subscripts c, r and cd refer to chains, rings and defect clusters, respectively.

ρ^*	Cycles/10^6	$\frac{U^*}{\mu^{*2}}$	$\bar{N}_c$	ϕ_c	$\bar{N}_r$	ϕ_r	$\bar{N}_{cd}$	ϕ_{cd}
0.025	20	−2.09	38	0.29	27	0.45	91	0.26
0.031 25	13	−2.09	42	0.29	28	0.42	91	0.29
0.037 5	13	−2.09	44	0.29	28	0.34	109	0.37
0.05	24	−2.09	45	0.28	28	0.28	119	0.44
0.062 5	22	−2.09	45	0.25	30	0.22	136	0.53
0.075	22	−2.09	44	0.22	30	0.18	162	0.60
0.1	18	−2.09	41	0.17	29	0.12	200	0.71
0.2	3	−2.10	19	0.02	22	0.03	1075	0.95

Finally, it is worth remarking that the model bears close connection with recent experiments [21, 76, 77] that report the observation of rings, chains and defects in monolayers of spherical monodispersed colloidal magnetic particles.

References

[1] Maleev S V 1966 *Sov. Phys.–JETP* **43** 1240
[2] De'Bell K, MacIsaac A B, Booth I N and Whitehead J P 1997 *Phys. Rev.* B **55** 15 108
[3] Rastelli E, Carbognani A, Regina S and Tassi A 1999 *J. Appl. Phys.* **85** 6082
[4] Mermin N D and Wagner H 1966 *Phys. Rev. Lett.* **71** 2729
[5] De'Bell K, MacIsaac A B and Whitehead J P 2000 *Rev. Mod. Phys.* **72** 225
[6] Hucht A and Usadel K D 1997 *Phys. Rev.* B **55** 12 309
[7] Allenspach R 1994 *J. Magn. Magn. Mater.* **129** 160 and references therein
[8] Politi P 1998 *Comments. Condens. Matter Phys.* **18** 191
[9] Seul M and Andelman D 1995 *Science* **267** 476
[10] McConnell H M, Tamm L K and Weis R M 1984 *Proc. Natl Acad. Sci. USA* **81** 3249
[11] Seul M and Sammon M J 1990 *Phys. Rev. Lett.* **64** 1903
[12] Seul M 1990 *Physica* A **168** 198
[13] Lösche M, Sackmann E and Möwald H 1990 *Ber. Bunsenges. Phys. Chem.* **87** 848
[14] McConnell H M 1991 *Annu. Rev. Phys. Chem.* **41** 171
[15] Kooy C and Enz U 1960 *Philips Res. Rep.* **15** 7
[16] Seul M and Wolfe R 1992 *Phys. Rev.* A **46** 7519
[17] Seshadri R and Westervelt R M 1992 *Phys. Rev.* B **46** 5142
[18] Faber T E 1958 *Proc. R. Soc.* A **248** 460
[19] Dormann J L, Fiorani D and Tronc E 1997 *Adv. Chem. Phys.* **98** 283
[20] Petit C, Taleb A and Pileni M P 1999 *J. Phys. Chem.* B **103** 1805
[21] Puntes V F, Krishnan K M and Alivisatos A P 2001 *Science* **291** 2115
[22] Puntes V F, Krishnan K M and Alivisatos A P 2001 *Appl. Phys. Lett.* **78** 2187
[23] Kusner R E, Mann J A and Dahm A J 1995 *Phys. Rev.* B **51** 5746
[24] Zahn K, Lenke R and Maret G 1999 *Phys. Rev. Lett.* **82** 2721
[25] Golosovsky M, Saado Y and Davidov D 1999 *Appl. Phys. Lett.* **75** 4168
[26] Wen W, Zhang L and Sheng P 2000 *Phys. Rev. Lett.* **85** 5464
[27] Kosterlitz J M and Thouless D J 1973 *J. Phys. C: Solid State Phys.* **6** 1181
[28] Nelson D R and Halperin B I 1979 *Phys. Rev.* B **19** 2457
[29] Young A P 1979 *Phys. Rev.* B **19** 1855
[30] Skjeltorp A T 1983 *Phys. Rev. Lett.* **51** 2306
[31] Helgesen G and Skjeltorp A T 1991 *Physica* A **180** 488
[32] Skjeltorp A T 1995 *Physica* A **213** 30
[33] Hurley M M and Singer S J 1992 *Phys. Rev.* B **46** 5783

[34] Hurley M M and Singer S J 1992 *J. Phys. Chem.* **96** 1938
[35] Hurley M M and Singer S J 1992 *J. Phys. Chem.* **96** 1951
[36] Taylor M B and Gyorffy B L 1993 *J. Phys.: Condens. Matter* **5** 4527
[37] Booth I, MacIsaac A B, Whitehead J P and De'Bell K 1995 *Phys. Rev. Lett.* **75** 950
[38] MacIsaac A B, Whitehead J P, De'Bell K and Poole P H 1996 *Phys. Rev. Lett.* **77** 739
[39] MacIsaac A B, De'Bell K and Whitehead J P 1998 *Phys. Rev. Lett.* **80** 616
[40] Stoycheva A D and Singer S J 2000 *Phys. Rev. Lett.* **84** 4657
[41] Stoycheva A D and Singer S J 2002 *Phys. Rev.* E **63** 036706
[42] Toxvaerd S 1998 *Mol. Phys.* **95** 539
[43] Hucht A, Moschel A and Usadel K D 1995 *J. Magn. Magn. Mater.* **148** 32
[44] Iglesias O and Labarta A 2000 *J. Magn. Magn. Mater.* **221** 149
[45] Weis J J 2002 *Mol. Phys.* **100** 579
[46] Garel T and Doniach S 1982 *Phys. Rev.* B **26** 325
[47] Andelman D, Brochard F and Joanny J-F 1987 *J. Chem. Phys.* **86** 3673
[48] Yafet Y and Gyorgy E M 1988 *Phys. Rev.* B **38** 9145
[49] Kashuba A and Pokrovsky V L 1993 *Phys. Rev.* B **48** 10 335
[50] Abanov Ar, Kalatsky V, Pokrovsky V L and Saslow W M 1995 *Phys. Rev.* B **51** 1023
[51] Chui S T 1995 *Phys. Rev. Lett.* **74** 3896
[52] Stoycheva A D and Singer S J 2001 *Phys. Rev.* E **64** 016118
[53] Néel L 1954 *J. Phys. Rad.* **15** 376
[54] Bruno P and Renard J P 1989 *Appl. Phys.* A **49** 499
[55] Schneider K P and Keller J 1997 *Chem. Phys. Lett.* **275** 63
[56] Weis J J 1998 *Mol. Phys.* **93** 361
[57] Zarragoicoechea G J 1999 *Mol. Phys.* **96** 1109
[58] Russier V 2001 *J. Appl. Phys.* **89** 1287
[59] Tavares J M, Weis J J and Telo da Gama M M 2002 *Phys. Rev.* E **65** 061201
[60] Gao G T, Zeng X C and Wang W 1997 *J. Chem. Phys.* **106** 3311
[61] de Gennes P G 1979 *Scaling Concepts in Polymer Physics* (Ithaca, NY: Cornell University Press)
[62] des Cloizeaux J and Jannink G 1990 *Polymers in Solution* (Oxford: Clarendon)
[63] Tlusty T and Safran S A 2000 *Science* **290** 1328
[64] Pincus P A 2000 *Science* **290** 1307
[65] Jund P, Kim S G, Tomanek D and Hetherington J 1995 *Phys. Rev. Lett.* **74** 3049
[66] Berretti A and Sokal A D 1985 *J. Stat. Phys.* **40** 483
[67] Tavares J M, Telo da Gama M M and Osipov M A 1997 *Phys. Rev.* E **56** R6252
[68] Teixeira P I C, Tavares J M and Telo da Gama M M 2000 *J. Phys.: Condens. Matter* **12** R411
[69] Wittmer J P, Milchev A and Cates M E 1998 *J. Chem. Phys.* **109** 834
[70] Wittmer J P, van der Schoot P, Milchev A and Barrat J L 2000 *J. Chem. Phys.* **113** 6992
[71] Camp P J, Shelley J C and Patey G N 2000 *Phys. Rev. Lett.* **84** 115
[72] Camp P J and Patey G N 2000 *Phys. Rev.* E **62** 5403
[73] Coniglio A 2001 *J. Phys.: Condens. Matter* **13** 9039
[74] Sear R P and Cuesta J 2001 *Europhys. Lett.* **55** 451
[75] Cuesta J A and Sear R P 2002 *Phys. Rev.* E **65** 031406
[76] Wen W, Pál K F, Zheng D W and Tu K N 1999 *Phys. Rev.* E **59** R4758
[77] Butter K, Philipse A P and Vroege G J 2002 *J. Magn. Magn. Mater.*